BL28XU
RISING II

1. Introduction

BL28XU is designed to realize technological innovations in batteries. Next-generation vehicles such as electric vehicles and plug-in hybrid vehicles are key technologies to reduce carbon dioxide emissions. The spread of these next-generation vehicles largely depends on the performance and safety of storage batteries. Therefore, the development of a post–lithium-ion battery with an energy density far greater than that of the current lithium-ion battery while maintaining the durability and life equivalency has attracted much attention. As part of the Research and Development Initiative for Scientific Innovation of New Generation Batteries (RISING2) project, Kyoto University has proposed four innovative storage battery systems: nano-interface–controlled batteries (halide shuttle batteries and conversion-type batteries), sulfide batteries, and zinc-air batteries. In addition, various advanced analysis tools for research on innovative storage batteries have been developed at BL28XU [1].

BL28XU mainly develops technology for *in situ* observations of the reaction inside storage batteries via the energy-dispersive confocal diffraction technique [2, 3], X-ray diffraction spectroscopy analysis [4-6], and hard X-ray photoelectron spectroscopy [7]. Since 2016, the RISING2 project has been ongoing as a contract research project of the New Energy and Industrial Technology Development Organization (NEDO) to promote technological advances for practical uses of storage batteries.

Based on the results of RISING, which was the predecessor of RISING2, research focuses on three subjects for storage batteries over a wide spatiotemporal scale: (1) elucidation of the reaction distribution generation factors, (2) analysis of active material reactions and non-equilibrium behaviors, and (3) elucidation of electrode/electrolyte interface phenomena. Our goal is to solve these subjects by developing technologies with sufficient spatial and time resolutions. In addition, the technologies to address the following subjects have been developed in the RISING2 project: (4) elucidation of the formation mechanism of random materials such as electrolytic solution and electrolytes at the electrode interface and (5) elucidation of thermodynamic or physical instability phenomena inside the storage batteries. Below representative achievements in FY2019 are reported.

2. Anomalous X-ray scattering experiment on a liquid electrolyte

Anomalous X-ray scattering (AXS) is a useful technique to clarify local structures around a specific element. In the case of a liquid electrolyte used for a battery, AXS may provide local structural information around metallic ions, which is closely related to various properties such as viscosity, solubility, and ionic conductivity. Therefore, structural insights obtained by AXS are important to design a superior electrolyte and improve battery performance. However, liquid electrolytes used for batteries have yet to be investigated with this technique due to the dilute concentration of the metallic ions in the electrolyte. In addition, the measurement time of AXS is typically more than a

few hours, which can induce X-ray radiation damage to the liquid sample.

To demonstrate the feasibility of the AXS method to liquid electrolytes, this technique was applied to 4 M KOH aqueous solution, which included 0.5 M of ZnO [8], a typical electrolyte used in alkaline batteries, silver oxide batteries, and zinc–air batteries. Note that the concentration of Zn^{2+} ion was only about 0.3 mol%.

Figure 1 shows pictures of the sample cells. When the KOH solution in the cell was irradiated with synchrotron X-rays, serious damage was observed in the Kapton X-ray windows (Fig. 1(a)). Therefore, polyether ether ketone (PEEK) films were adopted to seal the sample (Fig. 1(b)), which stably held the liquid sample throughout the AXS experiment. Additionally, to suppress the damage on the sample caused by the intense X-rays, the incident beam flux was set to ~3×10^{11} photons/s, which is about two orders of magnitude lower than the typical value in BL28XU.

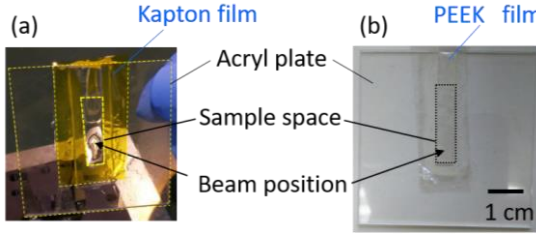

Fig. 1. Pictures of the sample cells. (a) Kapton and (b) PEEK films are used for the X-ray windows.

The scattered X-rays were recorded by the silicon drift detector at the incident X-ray energies of 9.637 keV (E_n) and 9.412 keV (E_f), which are 25 eV and 250 eV lower than the *K*-edge of the Zn^{2+} ion, respectively. The scan was repeated 27 times at E_n and E_f alternatively. The entire measurement required 40.5 h. Despite such a long irradiation time, the scattering patterns obtained at the first scan agreed well with those obtained at the last scan within the errors.

Figure 2 shows the obtained scattering patterns recorded at E_n and E_f. These scattering patterns almost overlap with each other, reflecting the dilute concentration of the Zn^{2+} ions. However, when comparing these patterns in more detail, a slightly lower intensity is observed for E_n than for E_f. This is the effect of the anomalous scattering term.

Figure 3(a) shows the differential structure factor

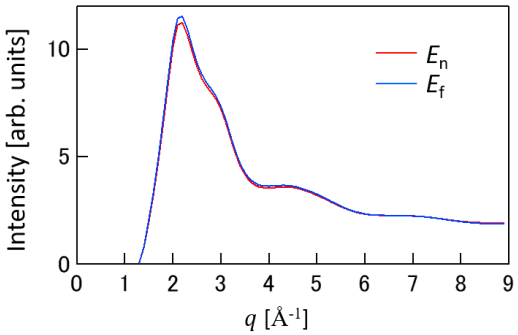

Fig. 2. Scattering patterns of 4 M KOH + 0.5 M ZnO aqueous solution measured at E_n and E_f.

$\Delta_{Zn}S(q)$ derived from the difference between the two scattering patterns in Fig. 2. Although the appearance of the $\Delta_{Zn}S(q)$ was noisy, an oscillatory pattern with peaks around 2.0 $Å^{-1}$ and 3.8 $Å^{-1}$ appeared, which was confirmed with the smoothed curve. Figure 3(b) shows the pair distribution function $\Delta_{Zn}G(r)$ obtained by the Fourier transformation of $\Delta_{Zn}S(q)$. The two peaks labeled as A and B were observed around 2.0 Å and 3.7 Å, respectively. While peak A corresponded to the Zn–O bond in the $[Zn(OH)_4]^{2-}$ anion species, peak B corresponded to the atomic correlations outside the $[Zn(OH)_4]^{2-}$ anion, indicating the formation of a polymeric species. The presence of a polymeric

species has been suggested by spectroscopic techniques, but the EXAFS technique has yet to detect any structural features corresponding to such species [9]. Consequently, AXS is more sensitive to medium-range correlations than EXAFS, and successfully detected peaks A and B.

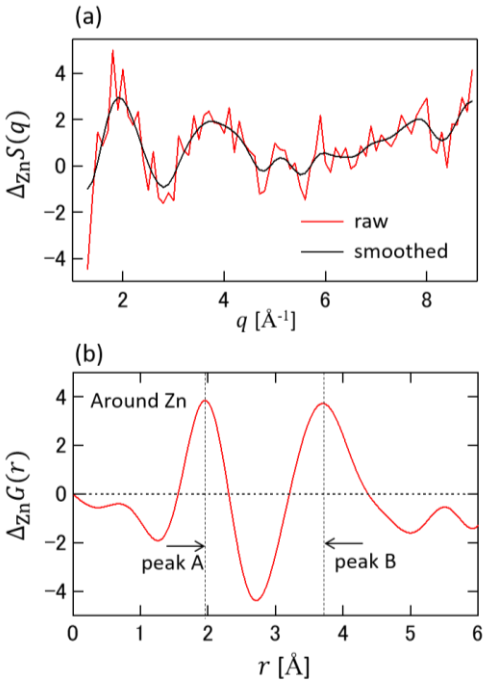

Fig. 3. (a) Differential structure factor $\Delta_{Zn}S(q)$ and (b) pair distribution function $\Delta_{Zn}(q)$ of the 4 M KOH + 0.5 M ZnO aqueous solution.

This work demonstrates the usefulness of the AXS technique for analyzing the local structure around dilute metallic ions. AXS should contribute to improved performances of batteries on the basis of the microscopic insight into metal complexes formed in the liquid electrolytes.

3. Development of operando hard X-ray photoelectron spectroscopy (HAXPES) system for an all-solid-state battery

A number of analytical methods have been used to clarify the charge–discharge mechanism of a lithium-ion battery and to improve its performance. Among them, operando analysis methods using XRD and XAFS have been realized in many synchrotron radiation facilities. However, operando XPS methods, which can observe the core level and valence bands, are rare because the probing depth is small (< several nm) and vacuum conditions are required. In FY2019, an operando HAXPES system for an all-solid-state battery was realized. This system can observe bulk-sensitive electronic states in electrode active materials due to the large probing depth (~10 nm to 50 nm) using photoelectrons excited by hard X-rays (> 6 keV) [10].

Figure 4(a) shows the dedicated bias-applied manipulator and sample holder for operando HAXPES measurements. A positive electrode $LiCoO_2$ was synthesized on a LICGC solid electrolyte substrate (OHARA) by pulsed laser deposition, and a current collector Al film was deposited thereon by electron beam evaporation. A buffer layer Li_3PO_4 and a negative electrode Li were laminated on the backside of the LICGC substrate by magnetron sputtering and resistance-heating vacuum evaporation, respectively. The operando HAXPES measurements were performed during galvanostatic charge–discharge tests between 3.0 V and 4.2 V.

Operando HAXPES successfully measured the reversible changes of the electronic states while charging and discharging the $LiCoO_2$ model thin film (Fig. 4(b)). In the Co 2*p* spectra, the main peak width at 780 eV and the satellite peak at 790 eV increased and decreased with charging, respectively, suggesting the valence changes from Co^{3+} to Co^{4+}. In the O 1*s* spectra, the peak derived from the lattice

oxygen of $LiCoO_2$ at 530 eV was split by charging, suggesting that oxygen anion contributes to the redox reaction. Therefore, operando HAXPES measurements can be a useful technique for analysis of reaction mechanisms for both anions and cations in active materials.

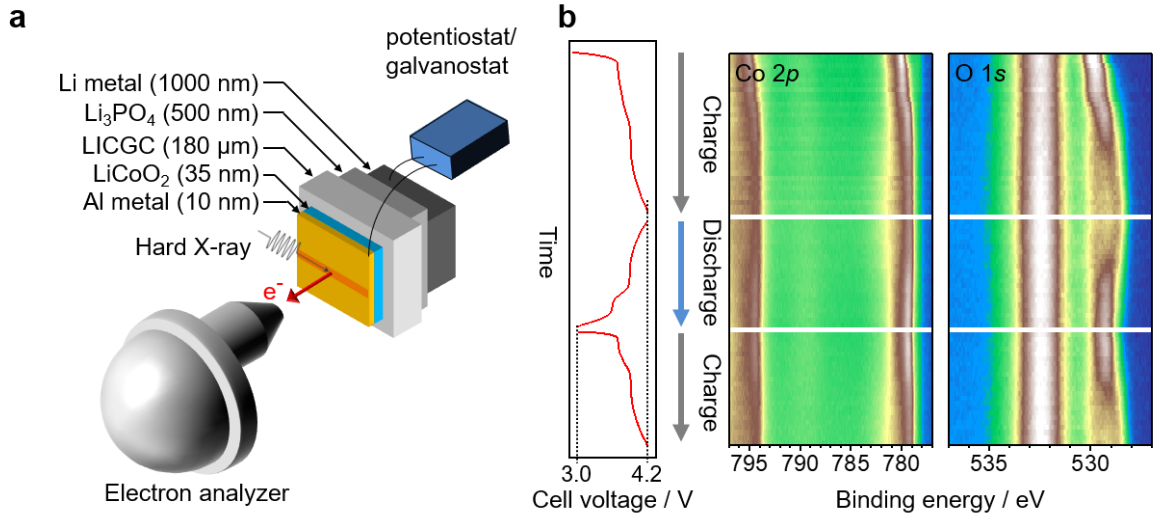

Fig. 4. (a) Schematic of the $LiCoO_2$ thin-film cell and the electrochemical setup for operando HAXPES. (b) Operando HAXPES spectra of Co 2*p* and O 1*s* during the 1st charge, 1st discharge, and 2nd charge of the $LiCoO_2$ thin-film cell.

Acknowledgments:

This work is based on the results of a project titled, "Research and Development Initiative for Scientific Innovation of New Generation Batteries (RISING2)", JPNP16001, commissioned by the New Energy and Industrial Technology Development Organization (NEDO).

Koji Kimura[*1] and Hisao Kiuchi[*2]

[*1] Department of Physical Science and Engineering, Nagoya Institute of Technology

[*2] Office of Society-Academia Collaboration for Innovation, Kyoto University

References:

[1] H. Tanida et al., *J. Synchrotron Radiat.* **21**, 268 (2014).

[2] H. Murayama et al., *J. Phys. Chem. C* **118**, 20750 (2014).

[3] H. Murayama et al., *Journal of JSSRR* **28**, 161 (2015).

[4] T. Kawaguchi et al., *J. Synchrotron Radiat.* **21**, 1247 (2014).

[5] T. Kawaguchi et al., *Phys. Chem. Chem. Phys.* **17**, 14064 (2015).

[6] T. Kawaguchi et al., *Journal of JSSRR* **28**, 124 (2015).

[7] K. Shimoda et al., *J. Mater. Chem. A* **4**, 5909 (2016).

[8] K. Kimura et al., *Anal. Chem* **92**, 9956 (2020).

[9] K. Pandya et al., *J. Phys. Chem.* **99**, 11976 (1995).

[10] H. Kiuchi et al., *Electrochem. Commun.* **118**, 106790 (2020).